

Kinetic and Mechanistic Studies of Carbon-to-Metal Hydrogen Atom Transfer Involving Os-Centered Radicals: Evidence for Tunneling

Anna Lewandowska-Andralojc,[†] David C. Grills,^{*,†} Jie Zhang,[†] R. Morris Bullock,^{*,‡} Akira Miyazawa,[§] Yuji Kawanishi,^{||} and Etsuko Fujita^{*,†}

[†]Chemistry Department, Brookhaven National Laboratory, Upton, New York 11973-5000, United States

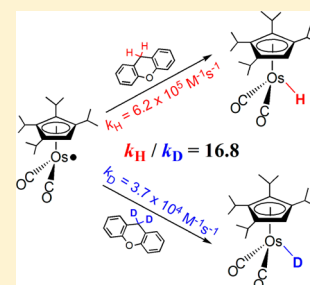
[‡]Physical Sciences Division, Pacific Northwest National Laboratory, P.O. Box 999, K2-57, Richland, Washington 99352, United States

[§]National Institute of Advanced Industrial Science and Technology, 4-2-1 Nigatake, Miyagino, Sendai, Miyagi 983-8551, Japan

^{||}National Institute of Advanced Industrial Science and Technology, Tsukuba Central 5, 1-1-1, Higashi, Tsukuba, Ibaraki, 305-8565, Japan

Supporting Information

ABSTRACT: We have investigated the kinetics of novel carbon-to-metal hydrogen atom transfer reactions, in which homolytic cleavage of a C–H bond is accomplished by a single metal-centered radical. Time-resolved IR spectroscopic measurements revealed efficient hydrogen atom transfer from xanthene, 9,10-dihydroanthracene, and 1,4-cyclohexadiene to Cp(CO)₂Os• and (η^5 -i-Pr₄C₅H)(CO)₂Os• radicals, formed by photoinduced homolysis of the corresponding osmium dimers. The rate constants for hydrogen abstraction from these hydrocarbons are in the range $1.5 \times 10^5 \text{ M}^{-1} \text{ s}^{-1}$ to $1.7 \times 10^7 \text{ M}^{-1} \text{ s}^{-1}$ at 25 °C. For the first time, kinetic isotope effects for carbon-to-metal hydrogen atom transfer were determined. Large primary deuterium kinetic isotope effects of 13.4 ± 1.0 and 16.8 ± 1.4 were observed for the hydrogen abstraction from xanthene to form Cp(CO)₂OsH and (η^5 -i-Pr₄C₅H)(CO)₂OsH, respectively, at 25 °C. Temperature-dependent measurements of the kinetic isotope effects over a 60 °C temperature range were carried out to obtain the difference in activation energies ($E_D - E_H$) and the pre-exponential factor ratio (A_H/A_D). For hydrogen atom transfer from xanthene to (η^5 -i-Pr₄C₅H)(CO)₂Os•, the ($E_D - E_H$) = $3.3 \pm 0.2 \text{ kcal mol}^{-1}$ and $A_H/A_D = 0.06 \pm 0.02$ values suggest a quantum mechanical tunneling mechanism.



INTRODUCTION

Hydrogen atom transfer (HAT) is one type of proton-coupled electron-transfer (PCET) reaction. PCET is a general term that includes reactions such as concerted proton electron transfer (CPET), consecutive electron–proton transfer (EPT), and consecutive proton–electron transfer (PET) reactions.¹ When a proton and an electron originate in the same orbital and move in a concerted manner to the same final orbital on another atom, the reaction can be called a HAT reaction. HAT reactions are fundamentally important in many types of chemical and biological processes. HATs from C–H bonds occur in the combustion of hydrocarbons, as well as in partial oxidation processes that are practiced industrially on a large scale. Radical reactions have been used for many years in organic synthetic methodology.² Many metal oxo complexes have been found to abstract a hydrogen atom from hydrocarbons. For example, extensive studies on cytochrome P450 show that an Fe=O complex abstracts a hydrogen atom as a key step in the oxidation process.³ The goal of selective oxidation of hydrocarbons has led to extensive studies of metalloenzyme complexes, particularly those of copper and iron.⁴ HATs from hydrocarbons to ruthenium oxo complexes⁵ and permanganate⁶ have been studied in detail, leading to the conclusion that the rates of these HAT reactions correlate with

the thermodynamics of the bonds being broken and formed, rather than directly correlating to localized spin density of the atom that will abstract the hydrogen atom.^{1c,7} Recent studies have reported the kinetics of HATs from hydrocarbons to the nitrogen atom of an iron imido complex.⁸

Transition metal hydrides are key reagents in many homogeneously catalyzed processes, and their reactivity as hydrogen atom donors has been extensively studied. The C=C bond of α -methylstyrene is readily hydrogenated by 2 equiv of HMn(CO)₅.⁹ The mechanism was shown to proceed by an initial HAT from the metal to the C=C bond, forming a carbon-centered radical. HAT from a second equivalent of HMn(CO)₅ to the carbon-centered radical generates the hydrogenated product. HATs from metal hydrides were also found to occur in the hydrogenation of substituted styrenes,¹⁰ anthracenes,¹¹ allenes,¹² and conjugated dienes.^{12,13} Evidence has been presented for HAT reactions in stoichiometric¹⁴ and catalytic¹⁵ hydroformylation reactions. The kinetics of HAT from a series of metal hydrides to a stabilized substituted trityl carbon-centered radical have been reported, providing insights

Received: December 3, 2013

Published: February 5, 2014

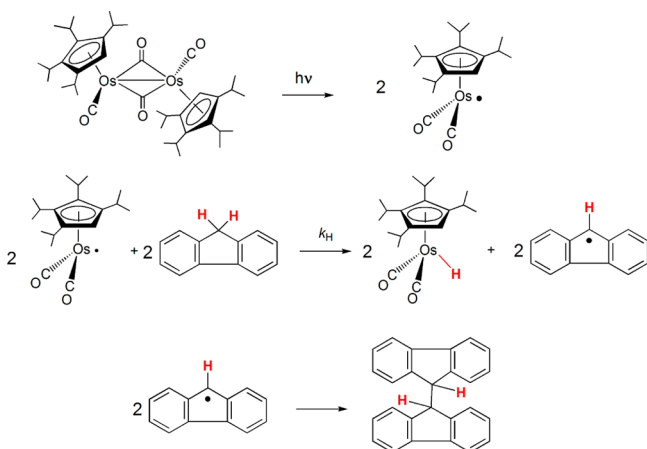
into the factors that govern the rates of HATs from metals to carbon-centered radicals.¹⁶

Wayland and co-workers found that Rh(II) complexes with bulky porphyrin ligands react with methane¹⁷ or toluene,¹⁸ cleaving the C–H bond and forming Rh–H and Rh–C bonds. These reactions had large negative entropies of activation, as expected for termolecular reactions involving a four-center transition state. Faster rates were found with bimetallo-radical Rh(II) complexes.¹⁹ These studies showed that metal-centered radicals were capable of reacting with C–H bonds, and the thermodynamics of those reactions were favorable due to formation of both a Rh–H and a Rh–C bond.

HATs from metals to carbon are generally thermodynamically favorable since C–H bonds are stronger than M–H bonds. However, since metals from the third row of the periodic table tend to form stronger bonds than those from the first or second row, we thought it might be possible for the opposite reaction to occur — HAT from a C–H bond to a metal-centered radical. We previously reported our initial studies showing the direct observation of carbon-to-metal HAT using time-resolved infrared (TRIR) spectroscopy.²⁰ Photochemical homolysis of the Os–Os bond of $[\text{Cp}(\text{CO})_2\text{Os}]_2$ ($\text{Cp} = \eta^5\text{-C}_5\text{H}_5$) generated the osmium-centered radical $\text{Cp}(\text{CO})_2\text{Os}^\bullet$, which abstracts a hydrogen atom from the C–H bond of 1,4-cyclohexadiene, producing the osmium hydride $\text{Cp}(\text{CO})_2\text{OsH}$.

We report here our extended studies of the kinetics of carbon-to-metal hydrogen atom transfers to $\text{Cp}(\text{CO})_2\text{Os}^\bullet$ and $(\eta^5\text{-}^i\text{Pr}_4\text{C}_5\text{H})(\text{CO})_2\text{Os}^\bullet$ (Scheme 1). We examined a range of organic substrates (shown in Chart 1) with different C–H bond dissociation energies (BDEs).²¹ For the first time, kinetic isotope effects (KIEs) were measured unambiguously for carbon-to-metal HAT.²² Large KIEs observed for abstraction of C–H vs C–D bonds, together with data obtained for the dependence of the KIEs on temperature, provide evidence for a quantum mechanical tunneling mechanism.

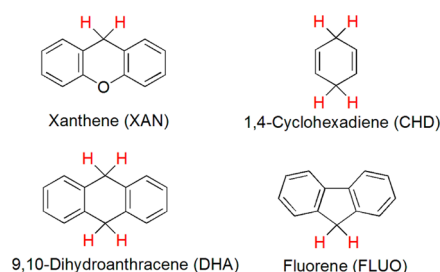
Scheme 1. Example of Photoinitiated HAT from Fluorene to $(\eta^5\text{-}^i\text{Pr}_4\text{C}_5\text{H})(\text{CO})_2\text{Os}^\bullet$



EXPERIMENTAL SECTION

General Procedures. All solutions were prepared in a nitrogen-filled MBraun glovebox. *n*-Heptane was purified by refluxing over CaH_2 followed by vacuum transfer onto NaK. After sitting over NaK, it was vacuum transferred to another vessel and used inside a glovebox. C_6D_6 was distilled from NaK. 9,10-Dihydroanthracene (DHA) was

Chart 1. Organic Hydrogen Atom Donors Used in This Study



purchased from Aldrich and recrystallized 5 times from ethanol to remove traces of anthracene. 1,4-Cyclohexadiene (CHD) was purchased from Aldrich and vacuum transferred from 4 Å molecular sieves before use. 9,9,10,10-Tetradeuterio-9,10-dihydroanthracene ($\text{DHA-}d_4$) (94.8% D) was synthesized according to a literature procedure.²³ Xanthene (XAN), fluorene (FLUO), and fluorene- d_{10} ($\text{FLUO-}d_{10}$) (99.1% D) of the best available purity were purchased from Aldrich and used without further purification. The synthetic procedure for 9,9-dideuterio-xanthene ($\text{XAN-}d_2$) (99.7% D) is described in the Supporting Information, SI. For the KIE determination based on continuous photolysis coupled with ^1H NMR measurements, two samples of $\text{XAN-}d_2$ with a lower % D content were prepared. The synthetic procedures and characterization of $[\text{Cp}(\text{CO})_2\text{Os}]_2$ and $[(\eta^5\text{-}^i\text{Pr}_4\text{C}_5\text{H})(\text{CO})_2\text{Os}]_2$ have been described previously.^{20,24}

Continuous Photolysis and KIE Measurements. Continuous photolysis was carried out in NMR tubes sealed with J. Young valves, and reaction progress was monitored by ^1H NMR spectroscopy. NMR spectra were obtained on a Bruker Avance III 400 FT NMR spectrometer (400 MHz for ^1H). Solutions of $[(\eta^5\text{-}^i\text{Pr}_4\text{C}_5\text{H})(\text{CO})_2\text{Os}]_2$ with hydrogen donors (XAN, $\text{XAN-}d_2$, FLUO, $\text{FLUO-}d_{10}$, $\text{DHA-}d_4$) in C_6D_6 were prepared under 1 atm N_2 and irradiated using UV–vis light generated from a 150 W xenon lamp with a low-energy pass filter ($\lambda > 300$ nm). The samples were held in a thermostatted cell holder. A series of deuterium labeling NMR experiments have been conducted to establish the KIE for the HAT reaction. For the measurements of the KIE dependence on temperature, the temperature was varied from 10 to 70 °C.

Measurement of the Rate of Hydrogen Atom Transfer. Time-resolved step-scan FTIR experiments were performed to identify the $\nu(\text{CO})$ band positions of the osmium species. The general procedure for this experiment is described in the SI. Time-resolved IR kinetic measurements were performed using a CW mode-hop-free external-cavity quantum cascade laser (QCL) (Daylight Solutions, 21052-MHF, 80 mW max. power) as a mid-IR probe source, and the third harmonic of a pulsed Nd:YAG laser (Continuum, Powerlite 7010, 355 nm, 5 ns) as the excitation source (details in SI). *n*-Heptane solutions of Os dimers were prepared at a concentration of 0.5–0.6 mM, with varying amounts of hydrogen atom donor (0–0.27 M), and transferred into an airtight CaF_2 IR cell (Harrick Scientific, DLC-S25, path length = 0.95 mm). The samples were held in a thermostatted cell holder with the temperature set to 25.0 °C.

Computational Details. DFT calculations were performed using the Gaussian 09 program (Revision B.01).²⁵ Geometry optimizations were performed using the default convergence criteria without any constraints. The B3LYP functional²⁶ was used together with the LANL2DZ ECP basis set²⁷ for Os and the 6-31G(d,p) basis set²⁸ for all other atoms. Frequency calculations were employed to characterize the stationary points as minima, to predict $\nu(\text{CO})$ IR frequencies, and to obtain thermochemical parameters for the estimation of the Os–H BDE.

RESULTS AND DISCUSSION

Carbon-to-Osmium Hydrogen Atom Transfer Reaction. In our previous work²⁰ it was shown that continuous

photolysis of $[\text{Cp}(\text{CO})_2\text{Os}]_2$ in C_6D_6 or THF- d_8 in the presence of excess 1,4-cyclohexadiene led to the formation of the osmium hydride, $\text{Cp}(\text{CO})_2\text{OsH}$ in 83–88% yield, together with benzene. Interestingly, the photolysis of $[\text{Cp}(\text{CO})_2\text{Os}]_2$ in the absence of CHD in THF also afforded $\text{Cp}(\text{CO})_2\text{OsH}$ in ~30% yield. The formation of $\text{Cp}(\text{CO})_2\text{OsH}$ in the absence of hydrogen donor was also observed directly in the TRIR experiment of an *n*-heptane solution of $[\text{Cp}(\text{CO})_2\text{Os}]_2$. In contrast to nearly all other known metal carbonyl radicals, $\text{Cp}(\text{CO})_2\text{Os}^\bullet$ radical does not cleanly dimerize back to the metal–metal bonded complex, but instead undergoes other reactions. A detailed analysis of these reactions falls beyond the scope of this paper and will be the subject of a future publication. In order to prevent such side reactions and limit the HAT reactions to those from added organic hydrogen atom donors such as CHD, an Os dimer in which the cyclopentadienyl ligands are substituted with four isopropyl groups, $[(\eta^5\text{-}i\text{-Pr}_4\text{C}_5\text{H})(\text{CO})_2\text{Os}]_2$, was prepared.

$[(\eta^5\text{-}i\text{-Pr}_4\text{C}_5\text{H})(\text{CO})_2\text{Os}]_2$ exhibits $\nu(\text{CO})$ IR bands at 1928 and 1730 cm^{-1} in *n*-heptane, indicating that it possesses both terminal and bridging CO ligands, as shown in Scheme 1. Laser flash photolysis ($\lambda_{\text{exc}} = 355 \text{ nm}$) of an *n*-heptane solution of $[(\eta^5\text{-}i\text{-Pr}_4\text{C}_5\text{H})(\text{CO})_2\text{Os}]_2$ leads to an instantaneous bleaching of the $\nu(\text{CO})$ IR bands of the dimer and the appearance of two new $\nu(\text{CO})$ bands at 1982 and 1917 cm^{-1} , as observed by nanosecond TRIR spectroscopy (Figure 1). The new bands are

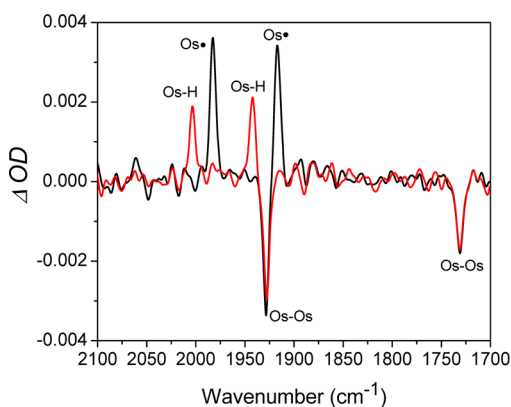


Figure 1. TRIR spectra obtained following 355 nm laser flash photolysis of $[(\eta^5\text{-}i\text{-Pr}_4\text{C}_5\text{H})(\text{CO})_2\text{Os}]_2$ (0.57 mM) and 1,4-cyclohexadiene (0.89 M) in *n*-heptane. Time delay: 200 ns (black), 15 μs (red).

assigned to the osmium-centered radical, $(\eta^5\text{-}i\text{-Pr}_4\text{C}_5\text{H})(\text{CO})_2\text{Os}^\bullet$. DFT computations predict $\nu(\text{CO})$ IR bands at 1981 and 1930 cm^{-1} , thus supporting the assignment of the transient species as $(\eta^5\text{-}i\text{-Pr}_4\text{C}_5\text{H})(\text{CO})_2\text{Os}^\bullet$. Based on the decay of the $\nu(\text{CO})$ bands of $(\eta^5\text{-}i\text{-Pr}_4\text{C}_5\text{H})(\text{CO})_2\text{Os}^\bullet$, this species lives ca. 100× longer than $\text{Cp}(\text{CO})_2\text{Os}^\bullet$. Formation of the hydride, $(\eta^5\text{-}i\text{-Pr}_4\text{C}_5\text{H})(\text{CO})_2\text{OsH}$, was not observed in the absence of a hydrogen atom donor (Figure S2).

In the analogous experiment but in the presence of CHD, the decay of the $\nu(\text{CO})$ bands due to $(\eta^5\text{-}i\text{-Pr}_4\text{C}_5\text{H})(\text{CO})_2\text{Os}^\bullet$ is concomitant with the simultaneous formation of two new bands at 2003 and 1943 cm^{-1} , assigned to $(\eta^5\text{-}i\text{-Pr}_4\text{C}_5\text{H})(\text{CO})_2\text{OsH}$ (Figure 1). The bands attributed to the osmium hydride grow at a rate identical to the rate of decay of the osmium radical (Figure 2). The assignment of the bands to $(\eta^5\text{-}i\text{-Pr}_4\text{C}_5\text{H})(\text{CO})_2\text{OsH}$ was based on a comparison to the IR

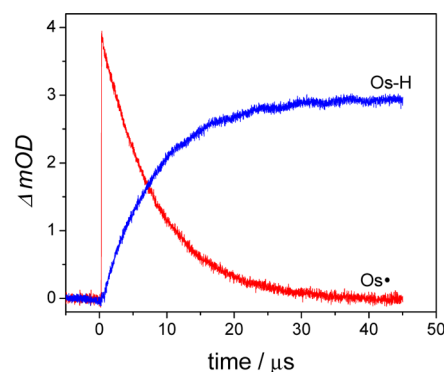


Figure 2. QCL TRIR kinetic traces obtained at the 1917 cm^{-1} band of $(\eta^5\text{-}i\text{-Pr}_4\text{C}_5\text{H})(\text{CO})_2\text{Os}^\bullet$ and the 1943 cm^{-1} band of $(\eta^5\text{-}i\text{-Pr}_4\text{C}_5\text{H})(\text{CO})_2\text{OsH}$ following 355 nm excitation of a 0.57 mM *n*-heptane solution of $[(\eta^5\text{-}i\text{-Pr}_4\text{C}_5\text{H})(\text{CO})_2\text{Os}]_2$ in the presence of 1,4-cyclohexadiene (0.89 M).

data reported earlier for the hydride that has been synthesized independently.²⁴ In this TRIR experiment, the hydrogen atom transfer reaction from carbon to metal, in which homolytic cleavage of a C–H bond is accomplished at a single metal center, was directly observed. Osmium forms stronger M–H bonds than most other transition metals,²⁹ which provides a driving force for this novel carbon-to-metal HAT reaction.

Kinetic Studies of the HAT Reaction. Since $(\eta^5\text{-}i\text{-Pr}_4\text{C}_5\text{H})(\text{CO})_2\text{Os}^\bullet$ performs efficient and clean HAT reactions from organic hydrogen donors, it offers a compelling opportunity to gain more insight into how this reaction proceeds. Carbon-to-metal hydrogen atom transfer rate constants were measured for hydrogen donors with different C–H BDEs (Table 1). In order to determine the HAT rate constants k_{H} , the decay of the osmium radical and growth of the osmium hydride were monitored in the presence of various concentrations of hydrogen donor.

A plot of pseudo-first-order rate constants for the osmium radical decay as a function of hydrogen donor concentrations gives a straight line, the slope of which provides the second-order rate constant, k_{H} , for carbon-to-metal hydrogen atom transfer (Table 2). Some illustrative examples of such derived plots are given in Figure 3 and SI Figure S3 and Figure S4. In the presence and absence of FLUO, no difference in the lifetime of the osmium radical was observed, indicating that hydrogen abstraction is not fast enough (see below) to be detected by time-resolved spectroscopy.

The observation of efficient hydrogen atom abstraction indicates that the reaction does not have a large thermochemical or kinetic barrier. The previously determined²⁰ Os–H BDE for $\text{Cp}(\text{CO})_2\text{Os–H}$ (BDE = 82 kcal mol^{-1}) and the newly calculated Os–H BDE for $(\eta^5\text{-}i\text{-Pr}_4\text{C}_5\text{H})(\text{CO})_2\text{Os–H}$ (BDE = 81 kcal mol^{-1}) indeed show that the Os–H bond is one of the strongest among metal hydride complexes. For comparison, the BDE of Ru–H in $\text{Cp}(\text{CO})_2\text{Ru–H}$ is 77 kcal mol^{-1} and the BDE of W–H in $\text{Cp}(\text{CO})_3\text{W–H}$ is 73 kcal mol^{-1} .^{29,33} The bond strengths thus provide a qualitative understanding of why these reactions occur. Hydrogen atom transfer from XAN, CHD, and DHA to the Os radical is a thermodynamically favorable process, since the Os–H BDE is stronger than the C–H BDEs of the hydrogen donors.

In general, the ability of a metal complex to abstract a hydrogen atom from a substrate correlates with the thermodynamic driving force for HAT. Bryant et al. reported

Table 1. BDEs for the C–H Bonds of the Hydrogen Donors and the Os–H Bonds of the Osmium Hydrides Used in the Study

compound	XAN	CHD	DHA	FLUO	Cp(CO) ₂ OsH	(η^5 -Pr ₄ C ₅ H)(CO) ₂ OsH
BDE (kcal mol ⁻¹)	75.5 ^a	73 ^b 77 ^c	78 ^a	80 ^a	82 ^c 80 ^f	81 ^d

^aRef 30. ^bRef 31, errors 2 kcal mol⁻¹. ^cRef 20 experimental data. ^dBased on our DFT calculations. ^eRevised value from ref 32. ^fRef 20 based on DFT calculations.

Table 2. Second-Order Rate Constants for HAT to Osmium Radicals, and the KIE of the Reaction

	$k_H / 10^5 \text{ M}^{-1} \text{ s}^{-1}$	$k_D / 10^5 \text{ M}^{-1} \text{ s}^{-1}$	KIE (k_H/k_D) ^b	KIE (¹ H NMR) ^c
		XAN		
Cp(CO) ₂ Os*	170 ± 10	13 ± 1	13.4 ± 1.0	-
(η^5 -Pr ₄ C ₅ H)(CO) ₂ Os*	6.2 ± 0.2	0.37 ± 0.03	16.8 ± 1.4	14.4 ± 0.9
		DHA		
Cp(CO) ₂ Os*	41 ± 3	-	-	-
(η^5 -Pr ₄ C ₅ H)(CO) ₂ Os*	2.1 ± 0.1	0.22 ± 0.09	9.3 ± 3.8	9.4 ± 0.6
		CHD		
Cp(CO) ₂ Os*	23 ± 2	-	-	-
(η^5 -Pr ₄ C ₅ H)(CO) ₂ Os*	1.5 ± 0.1	-	-	-
		FLUO		
Cp(CO) ₂ Os*	-	-	-	-
(η^5 -Pr ₄ C ₅ H)(CO) ₂ Os*	-	-	-	15.5 ± 1.8

^aAll data were determined at 25 °C. ^bKIE values were calculated based on unrounded rate constants. ^cKIE determined based on continuous photolysis followed by ¹H NMR measurements.

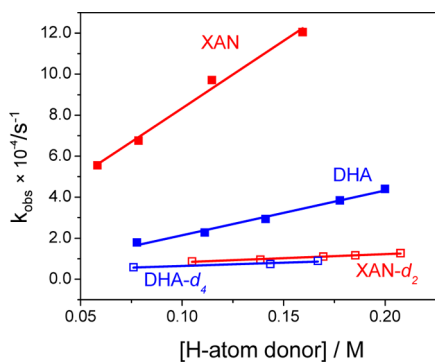


Figure 3. Plots of the observed rate constants for the decay of the (η^5 -Pr₄C₅H)(CO)₂Os* radical, k_{obs} , vs concentration of XAN (red, filled symbols), XAN- d_2 (red, open symbols), DHA (blue, filled symbols), and DHA- d_4 (blue, open symbols) following 355 nm excitation of 0.6 mM *n*-heptane solutions of [(η^5 -Pr₄C₅H)(CO)₂Os]₂.

that oxidation of a C–H bond by [(bpy)₂(py)Ru^{IV}O]²⁺ occurs by hydrogen atom abstraction followed by competitive radical dimerization and radical trapping by the oxidant.^{5a} It was found that the rate constants for the initial HAT step correlate well with the strength of the C–H bond being cleaved, over a range of 10⁵ in k .^{5a} That study encompassed both benzylic and allylic oxidations and included primary, secondary, and tertiary C–H bonds. Similarly, the rates of oxidation of alkylaromatic compounds by the manganese-oxo-phenanthroline dimers that proceed via HAT inversely correlate with the substrate C–H bond strength ($k_{\text{XAN}} > k_{\text{DHA}} > k_{\text{FLUO}}$).³⁴

However, in the case of carbon-to-osmium HAT, even if the obtained k_H values for both Os dimers (data in Table 2) are statistically corrected for the number of reactive hydrogens (e.g., 4 for DHA; 2 for XAN; 4 for CHD) the corrected order for k_H , k'_H (XAN) > k'_H (DHA) > k'_H (CHD) does not coincide with the BDE order, BDE_{XAN} (75.5 kcal/mol) < BDE_{CHD} (77 kcal/mol) < BDE_{DHA} (78 kcal/mol). The k'_H values obtained for xanthene are much higher than the k'_H

values predicted solely on the basis of the BDE of the C–H bond of xanthene, and the k'_H for DHA and CHD are reversed relative to their BDEs. This finding suggests that there are other factors in addition to the BDE of the C–H bond influencing the rate constant of the reaction. For example, a mechanistic study of HAT by an iron(III) imido complex revealed a strong dependence of the rate constants on the size and steric hindrance of the hydrocarbon substrate, e.g., the rate for CHD was about 90 times larger than for 1,4-dimethyl-1,4-cyclohexadiene, and 1,2,4,5-tetramethyl-1,4-cyclohexadiene did not undergo HAT although all three hydrocarbons have the same calculated BDE.⁸

HAT was not directly observed in the time-resolved spectroscopy experiment with FLUO. However, when continuous photolysis ($\lambda > 300 \text{ nm}$) of [(η^5 -Pr₄C₅H)(CO)₂Os]₂ was carried out in C₆D₆ in the presence of FLUO, after 27 min of irradiation all of the starting material was decomposed as monitored by ¹H NMR. The product formed could be attributed to the hydride, (η^5 -Pr₄C₅H)(CO)₂OsH, based on characteristic peaks of C₅–H at 4.82 ppm and Os–H at –13.69 ppm. In addition, ¹H NMR showed the formation of another organic product, which can be assigned to bifluorene (Scheme 1). The yield of bifluorene determined from the integration of ¹H NMR signals was found to be 100% based on the stoichiometry of the reaction, i.e., the fluorene radicals dimerize cleanly to form bifluorene. The analogous experiment was carried out for solutions of [(η^5 -Pr₄C₅H)(CO)₂Os]₂ with CHD. In that case, [(η^5 -Pr₄C₅H)(CO)₂Os]₂ is cleanly converted into (η^5 -Pr₄C₅H)(CO)₂OsH. ¹H NMR did show the formation of benzene with a yield of 78% based on the stoichiometry. We believe that benzene is formed by the disproportionation of cyclohexadienyl radicals that gives benzene and 1,4-cyclohexadiene.³⁵

H/D Kinetic Isotope Effect for the HAT Reaction. To gain further mechanistic details for the carbon-to-metal HAT, KIEs have been measured. Since the KIE values are large, the residual H contributes to the reactivity of the deuterated

materials. Taking this into account, but ignoring secondary isotope effects, the actual KIE ($k_{\text{H}}/k_{\text{D}}$) for the HAT from xanthene was determined from the measured values of the rate constants for hydrogen atom transfer, k_{H} and deuterium atom transfer with residual hydrogen atom transfer, $k_{\text{D,H}}$ (details in SI). The results yield a large primary KIE at 25 °C for the hydrogen abstraction from xanthene of 13.4 ± 1.0 and 16.8 ± 1.4 for $[\text{Cp}(\text{CO})_2\text{Os}]_2$ (Figure S5) and $[(\eta^5\text{-}i\text{-Pr}_4\text{C}_5\text{H})(\text{CO})_2\text{Os}]_2$, respectively (Figure 3).

Such significant KIEs prevent the accurate determination of the isotope effect using time-resolved spectroscopy for hydrogen donors with stronger C–H bonds than xanthene, i.e., with smaller k_{H} rate constants. An attempt has been made to obtain the KIE for the HAT from DHA to $(\eta^5\text{-}i\text{-Pr}_4\text{C}_5\text{H})(\text{CO})_2\text{Os}^*$, and it was found to be 9.3 ± 3.8 (Figure 3). The large KIE for HAT indicates that C–H bond breaking is an important part of the rate-limiting step. To further confirm the large KIE, a competitive method for the measurement of KIEs based on continuous photolysis combined with ^1H NMR reaction monitoring was applied. In this technique, both hydrogen and deuterium atom transfer reactions are carried out in the same vessel, minimizing systematic errors introduced through rate constants obtained from separate measurements. The measurements are based on the precise integration of the ^1H NMR peaks that correspond to $(\eta^5\text{-}i\text{-Pr}_4\text{C}_5\text{H})(\text{CO})_2\text{OsH}$ and $(\eta^5\text{-}i\text{-Pr}_4\text{C}_5\text{H})(\text{CO})_2\text{OsD}$ (details in SI).

This method is limited to $[(\eta^5\text{-}i\text{-Pr}_4\text{C}_5\text{H})(\text{CO})_2\text{Os}]_2$ because only this complex does not undergo HAT in the absence of a hydrogen donor. The KIE at 25 °C obtained for xanthene from the steady state measurement and ^1H NMR, $\text{KIE} = 14.4 \pm 0.9$, using xanthene- d_2 (97.5% D), is in reasonable agreement with the KIE obtained from the kinetic measurements ($\text{KIE} = 16.8 \pm 1.4$) using xanthene- d_2 (99.7% D). A similar magnitude of the KIE was obtained for FLUO (Table 2). Both techniques applied to obtain the KIE conclusively point to a large isotope effect for hydrogen atom transfer.

The results of kinetic isotope effect studies on the oxidation of hydrocarbons by transition metal complexes have also been reported.^{5a,36} A kinetic isotope effect of the magnitude of 35 was found for the HAT step in the oxidation of the C–H bond in DHA vs DHA- d_4 by $[(\text{bpy})_2(\text{py})\text{Ru}^{\text{IV}}\text{O}]^{2+}$.^{5a} An even higher KIE of 105 for the HAT step in the reaction of an iron(III) imido complex with CHD has been measured.⁸

The origin of the KIE arises from different zero point energies (ZPEs) between C–H and C–D. ZPEs are dependent on the frequency of the bond stretch, which is in turn dependent on the reduced mass of the two connected atoms. Using the semiclassical harmonic oscillator approximation and based on the mass difference of D and H, the KIE can easily be predicted to be ~ 6.4 at 20 °C. The KIE observed in this study, the first KIE determination for a carbon-to-metal H atom transfer reaction, in the range of 13–16 at 25 °C, is significantly greater than the semiclassical limit and cannot be accounted for solely by the differences in zero point energies.

Meyer and co-workers found a colossal kinetic isotope effect for PCET reactions in solution involving nitrogen, sulfur, and phosphorus as donors.³⁷ The highest value of KIE of 455 at 25 °C was reported for the reduction of benzoquinone to hydroquinone by the Os(IV) hydrazido complex, *trans*- $[\text{Os}^{\text{IV}}(\text{tpy})(\text{Cl})_2(\text{N}(\text{H})\text{N}(\text{CH}_2)_4\text{O})]\text{PF}_6$ (*tpy* = 2,2':6',2''-terpyridine). Based on the theory developed by Hammes-Schiffer,³⁸ the huge KIE was attributed to a relatively small

overlap between the reactant and product H or D vibrational wave functions arising from large hydrogen transfer distances.

Insight into the nature of the HAT reaction in our system was obtained from the application of the criteria for quantum mechanical tunneling that were established by Kreevoy in 1992.³⁹ The three Kreevoy criteria diagnostic of tunneling are (a) a kinetic isotope effect significantly larger than the ground-state zero-point energy, KIE minimum of 6.4 at 20 °C; (b) an activation energy difference ($E_{\text{D}} - E_{\text{H}}$) greater than 1.2 kcal mol⁻¹; and (c) a ratio of pre-exponential factors ($A_{\text{H}}/A_{\text{D}}$) less than 0.7. The first criterion simply requires the measurement of the KIE, while the second two criteria can be obtained from the measurement of the isotope effect as a function of temperature and, then, an Arrhenius plot of $\ln(\text{KIE})$ vs $1/T$. The value $E_{\text{D}} - E_{\text{H}}$ is obtained from the slope while $A_{\text{H}}/A_{\text{D}}$ is obtained from the intercept (see SI).

The three Kreevoy criteria have been used successfully by Klinman and by Finke in several different enzyme systems.⁴⁰ Temperature-dependent measurements of the deuterium KIE also implied a tunneling mechanism for reaction of $[(\text{bpy})_2(\text{py})\text{Ru}^{\text{IV}}\text{O}]^{2+}$ with H_2O vs D_2O ^{1e,41} or for HAT from ruthenium imidazole to TEMPO $^{\bullet}$ (2,2,6,6-tetramethylpiperidine-1-oxyl radical).⁴² It is also important to note that there are many metal-mediated HAT reactions that show modest KIEs.^{34,37a,43} For example, the isotope effect for transfer of a hydrogen/deuterium atom from $\text{H}_2\text{Os}(\text{CO})_4/\text{D}_2\text{Os}(\text{CO})_4$ to the monomeric trityl radical was reported to be only 4.3 at 25 °C.^{43c} There is, thus, diversity in the mechanisms of HAT reactions in terms of the tunneling contribution, and no simple pattern based on the structure or driving force is yet evident.

The $[(\eta^5\text{-}i\text{-Pr}_4\text{C}_5\text{H})(\text{CO})_2\text{Os}]_2$ system provides a unique opportunity to examine carbon-to-metal hydrogen and deuterium atom transfer reactions as a function of temperature. The dependence of $\ln(\text{KIE})$ vs $1/T$ was determined using steady-state irradiation combined with ^1H NMR measurements for a solution of $[(\eta^5\text{-}i\text{-Pr}_4\text{C}_5\text{H})(\text{CO})_2\text{Os}]_2$ in the presence of XAN- d_2 (97.5% D) (Figure 4) or FLUO- d_{10} (99.1% D) (Figure S7; Table S1). The obtained results from the analysis of the data from the plots of $\ln(\text{KIE})$ vs $1/T$ are summarized in Table 3.

The results reveal a large KIE for hydrogen atom transfer of 6.2 (70 °C) to 17.9 (10 °C) for XAN, and 9.8 (70 °C) to 18.0 (10 °C) for FLUO (Table 3). The values of the KIE, the activation energy difference ($E_{\text{D}} - E_{\text{H}}$), and the preexponential factor ratio, $A_{\text{H}}/A_{\text{D}}$, meet all three Kreevoy criteria, thus

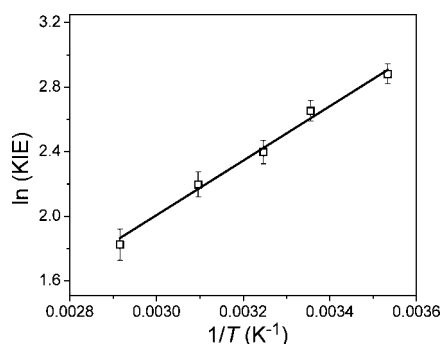


Figure 4. Plot of $\ln(\text{KIE})$ vs $1/T$ for hydrogen atom transfer reactions between $(\eta^5\text{-}i\text{-Pr}_4\text{C}_5\text{H})(\text{CO})_2\text{Os}^*$ and xanthene, obtained using XAN- d_2 (97.5% D). From the slope and intercept, the activation energy difference and the pre-exponential factor ratio were calculated.

Table 3. Summary of Data for the Dependence of KIE on Temperature for the Hydrogen Atom Transfer Reactions between (η^5 - i -Pr $_4$ C $_5$ H)(CO) $_2$ Os $^\bullet$ and XAN and FLUO

H-donor	temp range $^\circ\text{C}$	KIE	$E_D - E_H$ kcal mol $^{-1}$	A_H/A_D
tunneling criteria	—	>6.4 at 20 $^\circ\text{C}$	>1.2	<0.7
XAN	10–70	17.9–6.2	3.3 ± 0.2	0.06 ± 0.02
FLUO	10–70	18.0–9.8	2.0 ± 0.6	0.6 ± 0.3

signifying that tunneling plays a significant role in this reaction. In particular, for HAT from XAN to (η^5 - i -Pr $_4$ C $_5$ H)(CO) $_2$ Os $^\bullet$, the ($E_D - E_H$) = 3.3 ± 0.2 kcal mol $^{-1}$ and A_H/A_D = 0.06 ± 0.02 values indicate extensive tunneling for the H-atom transfer reaction. Of course, at least some tunneling is expected for such light-atom, net hydrogen atom transfers, with an increasing tunneling component to the observed rate at increasingly lower temperatures.

CONCLUSIONS

Time-resolved IR spectroscopy and steady-state irradiation studies have been used to elucidate the kinetic and mechanistic details of novel HAT reactions in which a hydrogen atom is transferred from a carbon to a metal center. In these reactions, homolytic cleavage of a C–H bond in a H-atom donor (1,4-cyclohexadiene, xanthene, 9,10-dihydroanthracene, or fluorene) is accomplished by a single metal-centered osmium radical that is generated by photoinduced Os–Os bond homolysis of an Os dimer ([Cp(CO) $_2$ Os] $_2$ or [(η^5 - i -Pr $_4$ C $_5$ H)(CO) $_2$ Os] $_2$). Second-order rate constants for HAT ranged from 1.5×10^5 M $^{-1}$ s $^{-1}$ to 1.7×10^7 M $^{-1}$ s $^{-1}$, depending on the strength of the C–H bond being cleaved and the nature of the Os radical, with the Cp(CO) $_2$ Os $^\bullet$ radical exhibiting rate constants approximately one order of magnitude larger than the (η^5 - i -Pr $_4$ C $_5$ H)(CO) $_2$ Os $^\bullet$ radical. We have also shown, for the first time, data for the KIE for carbon-to-metal hydrogen atom transfer. The two independent techniques applied to determine the KIE (time-resolved IR spectroscopy and ^1H NMR spectroscopy after steady-state irradiation) were in good agreement and revealed a large isotope effect for HAT, ranging from 9.3 to 16.8 at 25 $^\circ\text{C}$. Moreover, we have measured the k_H/k_D isotope effect data over a 60 $^\circ\text{C}$ temperature range, which allowed the activation energy differences and pre-exponential factor ratios to be calculated. For hydrogen atom transfer from xanthene to (η^5 - i -Pr $_4$ C $_5$ H)(CO) $_2$ Os $^\bullet$, the ($E_D - E_H$) = 3.3 ± 0.2 kcal mol $^{-1}$ and A_H/A_D = 0.06 ± 0.02 values support a significant quantum mechanical tunneling component in the mechanism for HAT from carbon-to-osmium radical.

ASSOCIATED CONTENT

Supporting Information

Experimental procedures for time-resolved IR spectroscopy and determination of HAT rate constants and kinetic isotope effects, and synthesis of XAN- d_2 . This material is available free of charge via the Internet at <http://pubs.acs.org>.

AUTHOR INFORMATION

Corresponding Authors

*E-mail: dcgrills@bnl.gov.

*E-mail: morris.bullock@pnnl.gov.

*E-mail: fujita@bnl.gov.

Present Address

Jie Zhang, School of Chemistry and Chemical Engineering, Henan Normal University, Xixiang, Henan 453007, China.

Notes

The authors declare no competing financial interest. Anna Lewandowska-Andralojc is on leave from the Faculty of Chemistry, Adam Mickiewicz University, Umultowska 89b, Poznan, Poland.

ACKNOWLEDGMENTS

The work at BNL was carried out under contract DE-AC02-98CH10886 with the U.S. Department of Energy and supported by its Division of Chemical Sciences, Geosciences & Biosciences, Office of Basic Energy Sciences. R.M.B. also thanks the U.S. Department of Energy, Office of Science, Office of Basic Energy Sciences, Division of Chemical Sciences, Geosciences & Biosciences for support. Pacific Northwest National Laboratory is operated by Battelle for the U.S. Department of Energy.

REFERENCES

- (1) (a) Weinberg, D. R.; Gagliardi, C. J.; Hull, J. F.; Murphy, C. F.; Kent, C. A.; Westlake, B. C.; Paul, A.; Ess, D. H.; McCafferty, D. G.; Meyer, T. J. *Chem. Rev.* **2012**, *112*, 4016–4093. (b) Savéant, J.-M. *Energy Environ. Sci.* **2012**, *5*, 7718–7731. (c) Mayer, J. M. *Acc. Chem. Res.* **2011**, *44*, 36–46. (d) Mayer, J. M. *Annu. Rev. Phys. Chem.* **2004**, *55*, 363–390. (e) Huynh, M. H. V.; Meyer, T. J. *Chem. Rev.* **2007**, *107*, 5004–5064.
- (2) Jasperse, C. P.; Curran, D. P.; Fevig, T. L. *Chem. Rev.* **1991**, *91*, 1237–1286.
- (3) Meunier, B.; de Visser, S. P.; Shaik, S. *Chem. Rev.* **2004**, *104*, 3947–3980.
- (4) Que, L.; Tolman, W. B. *Nature* **2008**, *455*, 333–340.
- (5) (a) Bryant, J. R.; Mayer, J. M. *J. Am. Chem. Soc.* **2003**, *125*, 10351–10361. (b) Matsuo, T.; Mayer, J. M. *Inorg. Chem.* **2005**, *44*, 2150–2158.
- (6) (a) Gardner, K. A.; Kuehnert, L. L.; Mayer, J. M. *Inorg. Chem.* **1997**, *36*, 2069–2078. (b) Gardner, K. A.; Mayer, J. M. *Science* **1995**, *269*, 1849–1851.
- (7) Mayer, J. M. *Acc. Chem. Res.* **1998**, *31*, 441–450.
- (8) Cowley, R. E.; Eckert, N. A.; Vaddadi, S.; Figg, T. M.; Cundari, T. R.; Holland, P. L. *J. Am. Chem. Soc.* **2011**, *133*, 9796–9811.
- (9) Sweany, R. L.; Halpern, J. J. *Am. Chem. Soc.* **1977**, *99*, 8335–8337.
- (10) (a) Nalesnik, T. E.; Freudenberger, J. H.; Orchin, M. *J. Mol. Catal.* **1982**, *16*, 43–49. (b) Nalesnik, T. E.; Orchin, M. *Organometallics* **1982**, *1*, 222–223. (c) Bullock, R. M.; Samsel, E. G. *J. Am. Chem. Soc.* **1990**, *112*, 6886–6898.
- (11) (a) Feder, H. M.; Halpern, J. J. *Am. Chem. Soc.* **1975**, *97*, 7186–7188. (b) Sweany, R. L.; Comberrel, D. S.; Dombourian, M. F.; Peters, N. A. *J. Organomet. Chem.* **1981**, *216*, 57–63.
- (12) Garst, J. F.; Bockman, T. M.; Batlaw, R. J. *Am. Chem. Soc.* **1986**, *108*, 1689–1691.
- (13) Shackleton, T. A.; Baird, M. C. *Organometallics* **1989**, *8*, 2225–2232.
- (14) (a) Nalesnik, T. E.; Orchin, M. *J. Organomet. Chem.* **1981**, *222*, C5–C8. (b) Ungváry, F.; Markó, L. *Organometallics* **1982**, *1*, 1120–1125.
- (15) Klingler, R. J.; Rathke, J. W. *J. Am. Chem. Soc.* **1994**, *116*, 4772–4785.
- (16) Eisenberg, D. C.; Lawrie, C. J. C.; Moody, A. E.; Norton, J. R. *J. Am. Chem. Soc.* **1991**, *113*, 4888–4895.

- (17) Sherry, A. E.; Wayland, B. B. *J. Am. Chem. Soc.* **1990**, *112*, 1259–1261.
- (18) Wayland, B. B.; Ba, S.; Sherry, A. E. *J. Am. Chem. Soc.* **1991**, *113*, 5305–5311.
- (19) (a) Cui, W.; Wayland, B. B. *J. Am. Chem. Soc.* **2004**, *126*, 8266–8274. (b) Cui, W.; Zhang, X. P.; Wayland, B. B. *J. Am. Chem. Soc.* **2003**, *125*, 4994–4995. (c) Zhang, X.-X.; Wayland, B. B. *J. Am. Chem. Soc.* **1994**, *116*, 7897–7898.
- (20) Zhang, J.; Grills, D. C.; Huang, K.-W.; Fujita, E.; Bullock, R. M. *J. Am. Chem. Soc.* **2005**, *127*, 15684–15685.
- (21) The bond dissociation energy is defined as the standard enthalpy change when a bond is cleaved by homolysis, with all reactants and products at 0 K.
- (22) In this paper, the abbreviation HAT refers to both hydrogen and deuterium atom transfers.
- (23) Mayr, H.; Lang, G.; Ofial, A. R. *J. Am. Chem. Soc.* **2002**, *124*, 4076–4083.
- (24) Zhang, J.; Huang, K.-W.; Szalda, D. J.; Bullock, R. M. *Organometallics* **2006**, *25*, 2209–2215.
- (25) Frisch, M. J.; et al. *Gaussian 09*, revision B.01; Gaussian, Inc.: Wallingford, CT, 2010.
- (26) (a) Becke, A. D. *J. Chem. Phys.* **1993**, *98*, 5648–5652. (b) Stephens, P. J.; Devlin, F. J.; Chabalowski, C. F.; Frisch, M. J. *J. Phys. Chem.* **1994**, *98*, 11623–11627.
- (27) (a) Hay, P. J.; Wadt, W. R. *J. Chem. Phys.* **1985**, *82*, 299–310. (b) Hay, P. J.; Wadt, W. R. *J. Chem. Phys.* **1985**, *82*, 270–283. (c) Wadt, W. R.; Hay, P. J. *J. Chem. Phys.* **1985**, *82*, 284–298.
- (28) (a) Francl, M. M.; Pietro, W. J.; Hehre, W. J.; Binkley, J. S.; Gordon, M. S.; DeFrees, D. J.; Pople, J. A. *J. Chem. Phys.* **1982**, *77*, 3654–3665. (b) Hariharan, P. C.; Pople, J. A. *Theoret. Chim. Acta* **1973**, *28*, 213–222.
- (29) Tilset, M.; Parker, V. D. *J. Am. Chem. Soc.* **1989**, *111*, 6711–6717; as modified in *J. Am. Chem. Soc.* **1990**, *112*, 2843.
- (30) Bordwell, F. G.; Cheng, J.; Ji, G. Z.; Satish, A. V.; Zhang, X. J. *Am. Chem. Soc.* **1991**, *113*, 9790–9795.
- (31) Burkey, T. J.; Majewski, M.; Griller, D. *J. Am. Chem. Soc.* **1986**, *108*, 2218–2221.
- (32) Laarhoven, L. J. J.; Mulder, P.; Wayner, D. D. M. *Acc. Chem. Res.* **1999**, *32*, 342–349.
- (33) Estes, D. P.; Vannucci, A. K.; Hall, A. R.; Lichtenberger, D. L.; Norton, J. R. *Organometallics* **2011**, *30*, 3444–3447.
- (34) Larsen, A. S.; Wang, K.; Lockwood, M. A.; Rice, G. L.; Won, T.-J.; Lovell, S.; Sadilek, M.; Turecek, F.; Mayer, J. M. *J. Am. Chem. Soc.* **2002**, *124*, 10112–10123.
- (35) (a) James, D. G. L.; Suart, R. D. *Chem. Commun.* **1966**, 484–485. (b) Studier, M. H.; Hart, E. J. *J. Am. Chem. Soc.* **1969**, *91*, 4068–4072.
- (36) Stultz, L. K.; Huynh, M. H. V.; Binstead, R. A.; Curry, M.; Meyer, T. J. *J. Am. Chem. Soc.* **2000**, *122*, 5984–5996.
- (37) (a) Huynh, M. H. V.; Meyer, T. J. *Proc. Natl. Acad. Sci. U.S.A.* **2004**, *101*, 13138–13141. (b) Huynh, M. H. V.; Meyer, T. J.; White, P. S. *J. Am. Chem. Soc.* **1999**, *121*, 4530–4531. (c) Huynh, M.-H. V.; White, P. S.; Meyer, T. J. *Angew. Chem., Int. Ed. Engl.* **2000**, *39*, 4101–4104. (d) Roecker, L.; Meyer, T. J. *J. Am. Chem. Soc.* **1987**, *109*, 746–754.
- (38) (a) Decornez, H.; Hammes-Schiffer, S. *J. Phys. Chem. A* **2000**, *104*, 9370–9384. (b) Iordanova, N.; Hammes-Schiffer, S. *J. Am. Chem. Soc.* **2002**, *124*, 4848–4856. (c) Soudackov, A.; Hammes-Schiffer, S. *J. Chem. Phys.* **1999**, *111*, 4672–4687.
- (39) (a) Kim, Y.; Kreevoy, M. M. *J. Am. Chem. Soc.* **1992**, *114*, 7116–7123. (b) Kwart, H. *Acc. Chem. Res.* **1982**, *15*, 401–408.
- (40) (a) Doll, K. M.; Finke, R. G. *Inorg. Chem.* **2003**, *42*, 4849–4856. (b) Kohen, A.; Klinman, J. P. *Acc. Chem. Res.* **1998**, *31*, 397–404. (c) Tsai, S.-c.; Klinman, J. P. *Biochemistry* **2001**, *40*, 2303–2311.
- (41) Binstead, R. A.; Meyer, T. J. *J. Am. Chem. Soc.* **1987**, *109*, 3287–3297.
- (42) Wu, A.; Mayer, J. M. *J. Am. Chem. Soc.* **2008**, *130*, 14745–14754.
- (43) (a) Gardner, K. A.; Kuehnert, L. L.; Mayer, J. M. *Inorg. Chem.* **1997**, *36*, 2069–2078. (b) Roth, J. P.; Lovell, S.; Mayer, J. M. *J. Am. Chem. Soc.* **2000**, *122*, 5486–5498. (c) Rodkin, M. A.; Abramo, G. P.; Darula, K. E.; Ramage, D. L.; Santora, B. P.; Norton, J. R. *Organometallics* **1999**, *18*, 1106–1109.